Z_4 to U(1) crossover of the order-parameter symmetry in a two-dimensional valence-bond solid

Jie Lou and Anders W. Sandvik
Department of Physics, Boston University, 590 Commonwealth Avenue, Boston, Massachusetts 02215, USA
(Received 29 July 2009; revised manuscript received 5 November 2009; published 31 December 2009)

We discuss ground-state projector simulations of a modified two-dimensional $S=1/2$ Heisenberg model in the valence bonds basis. Tuning matrix elements corresponding to the diagonal and off-diagonal terms in the quantum dimer model, we show that there is a quantum phase transition from the antiferromagnet into a columnar valence-bond solid (VBS). There are no signs of discontinuities, suggesting a continuous or very weak first-order transition. The Z_4-symmetric VBS order parameter exhibits an emergent U(1) symmetry as the phase transition is approached. We extract the associated length-scale governing the $U(1)-Z_4$ cross-over inside the VBS phase.

DOI: 10.1103/PhysRevB.80.212406 PACS number(s): 75.10.Jm, 75.40.Cx, 75.40.Mg, 64.70.Tg

A valence-bond solid (VBS) is a magnetically disordered state of a quantum spin system in which translational symmetry is spontaneously broken due to the formation of a pattern of strong and weak bond correlations $\langle \mathbf{S}_i \cdot \mathbf{S}_j \rangle$ (where i,j are nearest-neighbor sites). Using an SU(N) generalization of the Heisenberg model, Read and Sachdev showed that a fourfold degenerate columnar VBS ground state can be expected on the square lattice.[1] Numerical studies have found evidence for such VBS states in frustrated SU(2) symmetric systems,[2] but because of technical limitations, in particular the sign problem in quantum Monte Carlo (QMC) simulations,[3] the nature of the strongly frustrated ground state remains controversial.[4] Another challenging issue is how the ground state evolves from an antiferromagnet (AF) into a VBS. According to the "Landau rules," one would expect a direct transition between these states to be first-order,[5] because unrelated symmetries are broken. There could also be an intervening disordered (spin liquid) phase[6] or a coexistence region. Senthil *et al.* recently suggested an alternative scenario for a generic continuous transition based on a "deconfined" quantum critical point (DQCP) associated with spinon deconfinement.[7,8] This proposal has generated significant interest, as well as controversy. An extended "J-Q" Heisenberg model has been introduced,[9] which is not frustrated, in the standard sense, but includes a four-spin interaction which destroys the AF order and leads to a VBS ground state. This model is amenable to large scale QMC studies, which show scaling behavior consistent with a DQCP.[9,10] Other studies dispute these findings, however.[11] Numerical studies of the proposed field theory describing the deconfined quantum critical point are also subject to conflicting interpretations.[12,13] Further studies of AF-VBS transitions is thus called for.

In this Brief Report, we address an important aspect of the VBS state and the AF-VBS transition, namely, the nature of the quantum fluctuations of the VBS order parameter. In the DQCP theory, the Z_4 symmetric lattice-imposed structure of the VBS is a dangerously irrelevant, and, as a consequence, U(1) symmetry emerges close to the DQCP.[7] A U(1) symmetric VBS order parameter was indeed confirmed in the studies of the J-Q model,[9–11] and also in simulations of the SU(N) Heisenberg model with $N>4$.[14] However, the expected cross-over into a Z_4 symmetric distribution inside the VBS phase was not observed. This can be interpreted as the lattice sizes studied so far being smaller than the spinon confinement length scale Λ, which governs the $U(1)-Z_4$ cross-over.[15] Λ should diverge as ξ_d^a, where ξ_d is the dimer (VBS) correlation length and $a>1$,[7] and for a finite lattice with $L \ll \Lambda$ the distribution should be U(1) symmetric. The models studied so far have a rather weak VBS order, and hence ξ_d is large, which likely makes it difficult to satisfy $L \gg \xi_d^a$. The exponent a is not known.

Here, we introduce a way to generate much more robust VBS states, with which we can study the $U(1)-Z_4$ crossover already on small lattices. Our approach is based on a ground-state projector QMC method operating in the valence bond (VB) basis.[16–18] Starting from some trial state $|\Psi\rangle$, the ground state of a Hamiltonian H can be obtained by applying a high power of H; $|\Psi_0\rangle \sim H^m|\Psi\rangle$. Consider the $S=\frac{1}{2}$ Heisenberg model written as a sum of singlet projection operators H_{ij},

$$H = -J\sum_{\langle i,j\rangle} H_{ij}, \quad H_{ij} = \frac{1}{4} - \mathbf{S}_i \cdot \mathbf{S}_j, \tag{1}$$

where $\langle i,j\rangle$ denotes nearest neighbors on a square lattice of $N=L^2$ sites. In the VB basis the trial state $|\Psi\rangle$ is a superposition of singlet products $|(a_1,b_1)\cdots(a_{N/2},b_{N/2})\rangle$, where $(a,b)=(\uparrow_a\downarrow_b-\downarrow_a\uparrow_b)/\sqrt{2}$ with a and b sites on different sublattices. We here use the amplitude-product state of Liang *et al.*[19,20] A singlet projector can have two different effects upon acting on a VB state,

$$H_{ab}|\cdots(a,b)(c,d)\cdots\rangle = 1|\cdots(a,b)(c,d)\cdots\rangle, \tag{2}$$

$$H_{ad}|\cdots(a,b)(c,d)\cdots\rangle = \frac{1}{2}|\cdots(a,d)(c,b)\cdots\rangle. \tag{3}$$

These rules form the basis of the VB projector method,[16–18] where H^m is expanded in its strings of m singlet projectors. Expectation values of operators O are obtained by importance-sampling the VBs and operator strings produced when expanding

$$\langle O\rangle = \frac{\langle\Psi|H^m O H^m|\Psi\rangle}{\langle\Psi|H^m H^m|\Psi\rangle}. \tag{4}$$

For details of these procedures we refer to Refs. 16 and 17.

In Ref. 9, the J-Q model, which includes a four-spin cou-

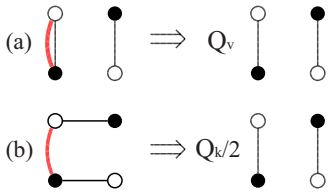

FIG. 1. (Color online) Diagonal (a) and off-diagonal (b) singlet projection operations (indicated by the arches) on VB pairs on a plaquette. The matrix elements (2) and (3) corresponding to these operations are multiplied by Q_v and Q_k, respectively. In (a), the factor is $2Q_v$ if there is a VB also on the left side of the operator. For all other bond configurations the matrix elements remain those in Eqs. (2) and (3).

pling consisting of terms $-QH_{ij}H_{kl}$, with ij and kl site pairs on two opposite edges of a plaquette, was studied using the VB projector method. The Q term naturally favors singlet formation on plaquettes, and this was shown to lead to a VBS state when $J/Q<(J/Q)_c$, $(J/Q)_c \approx 0.04$. Here, we introduce another mechanism leading to VBS formation. We define an effective Hamiltonian based on the Heisenberg model in the VB basis, by changing the diagonal matrix element 1 in Eq. (2) and the off-diagonal matrix element $\frac{1}{2}$ in Eq. (3) to Q_v and $\frac{1}{2}Q_k$, respectively, for H_{ab} acting on VBs on opposite edges of the same plaquette. These operations, illustrated in Fig. 1, correspond to the kinetic and potential-energy terms of the quantum dimer model.[21] There, however, the Hilbert space consists of only dimers connecting nearest-neighbor sites, whereas we here keep the full space of VBs connecting any pair of sites on different sublattices. In the quantum dimer model, the dimer configurations are also considered as orthogonal states, whereas we here keep the singlet nature of the VBs, whence the states are non-orthogonal. The nonorthogonality may at first sight seem problematic, because when $Q_v, Q_k \neq 1$ the Hamiltonian is non-Hermitian. We therefore refer to it as an *pseudo Hamiltonian* in the VB basis. However, in spite of this, the states generated by the projection procedure (with the sampling weights modified by the presence of the factors Q_v and Q_k, and taking the power m large enough for convergence to the $m=\infty$ limit) are completely well-defined SU(2) invariant quantum states. We can thus think of the modified projection technique as a means of generating a family of states parametrized by Q_v and Q_k. Moreover, there must be some corresponding Hamiltonians, defined in terms of the standard spin operators $\mathbf{S}_i$, which have these states as their ground states. Although we are not able to write down these Hamiltonians (which likely contain multispin interactions, possibly long ranged), it is still useful to study the evolution of the states as a function of Q_v and Q_k. Here we will consider two cases; $Q_v \geq 1$, $Q_k=1$ and $Q_k \geq 1$, $Q_v=1$, which we refer to as the Q_v and Q_k models, respectively. Both these models indeed undergo AF-VBS transitions.

We calculate the square of the staggered magnetization, $M^2=\langle \mathbf{M}\cdot\mathbf{M}\rangle$, where

$$\mathbf{M} = \frac{1}{N}\sum_{x,y} (-1)^{x+y}\mathbf{S}_{x,y} \tag{5}$$

is the operator for the AF order parameter. The columnar VBS operator for x-oriented bonds is

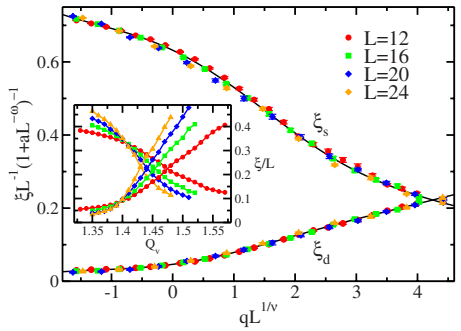

FIG. 2. (Color online) Finite-size scaling of the spin and dimer correlation lengths. The inset shows ξ/L versus the coupling, with crossing points tending toward $Q_v^c \approx 1.40$.

$$D_x = \frac{1}{N}\sum_{x,y} (-1)^x \mathbf{S}_{x,y}\cdot\mathbf{S}_{x+1,y}, \tag{6}$$

and D_y is defined analogously. We calculate the squared order parameter, $D^2=\langle D_x^2+D_y^2\rangle$, and the distribution $P(D_x,D_y)$ as in Ref. 9. Results for these quantities and the corresponding spin and dimer correlation lengths ξ_s (spin) and ξ_d (defined through the momentum-space second moments of the spin and dimer correlation functions) indicate coinciding critical points for the AF and VBS order parameters. In the following, we first discuss the finite size scaling behavior of the Q_v model.

We define a reduced coupling $q=Q_v-Q_v^c$. Then, if there indeed is a single critical point, there is AF order for $q<0$ and VBS order for $q>0$, and in the thermodynamic limit the squared spin and dimer order parameters should scale as $M^2 \sim (-q)^{2\beta_s}$ and $D^2 \sim q^{2\beta_d}$ inside the respective phases. To extract Q_v^c and the exponents, we use standard finite-size scaling forms,

$$M^2 = L^{-\sigma_s}(1+aL^{-\omega})F_s(qL^{1/\nu}), \tag{7}$$

$$D^2 = L^{-\sigma_d}(1+aL^{-\omega})F_d(qL^{1/\nu}), \tag{8}$$

$$\xi_{s,d} = L(1+aL^{-\omega})G_{s,d}(qL^{1/\nu}), \tag{9}$$

where $\sigma_s=2\beta_s/\nu$, $\sigma_d=2\beta_d/\nu$, and the correlation length exponent ν is the same for all the quantities (as also required in the DQCP theory). The scaling functions $F_{s,d}$ and $G_{s,d}$ are extracted in the standard way by adjusting the critical point and exponents to collapse finite-size data onto common curves. Since our lattices are not very large, $L \leq 24$, a subleading correction helps significantly to scale the data. In all cases we find that $\omega=1$ works well (the prefactor a is quantity-dependent, however).

Results are shown in Figs. 2 and 3. All the data can be scaled with $Q_v^c=1.400(5)$, $\nu=0.78(3)$, $\beta_s=0.27(2)$, and $\beta_d=0.68(3)$. Here, ν and β_d are approximately the same, within error bars, as in the J-Q model,[9] while β_s is much smaller (in the J-Q model $\beta_s>0.6$ was found[9,10]). The range of system sizes is quite small and we cannot, of course, exclude drifts in the exponents for larger lattices, nor a very weakly first-order transition.

Turning to the Q_k model, it is more demanding computa-

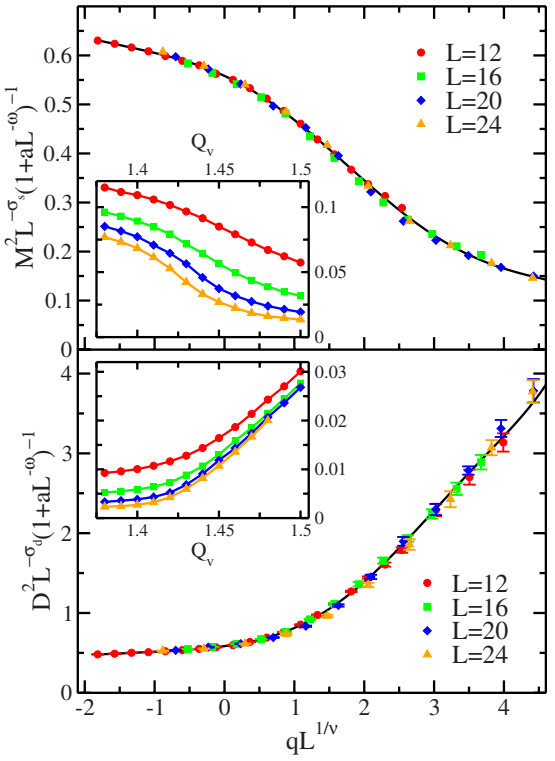

FIG. 3. (Color online) Finite size scaling of the squared AF (top panel) and VBS (bottom panel) order parameters of the Q_v model. The insets show the unscaled data.

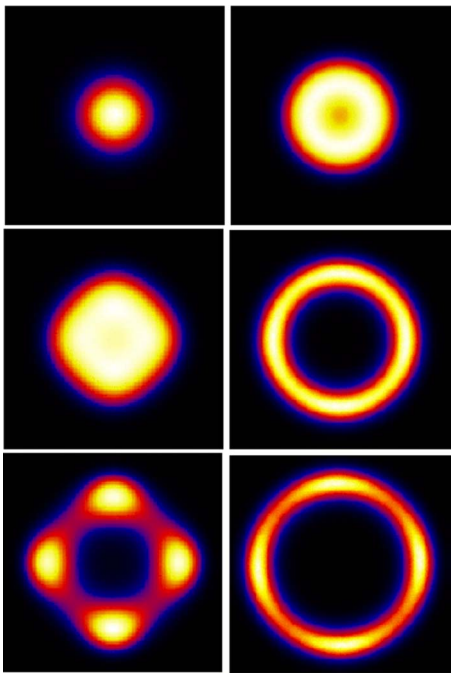

FIG. 4. (Color online) VBS order=parameter distributions. The left column is for $Q_k=1$ and $Q_v=1.44$, 1.48, and 1.54 (from top) on 12×12 lattices. The right column is for $Q_v=1$ and $Q_k=2.5$, 3.5, and 5.0 (from top) on 16×16 lattices.

tionally, because the critical point is rather large, $Q_k=2.5(1)$, leading to a lower acceptance rate in simulations close to the transition than for the Q_v model. We can therefore not reach the same level of precision for the exponents. The results are nevertheless consistent with a continuous transition and exponents similar to those of the Q_v model.

Unfortunately, we cannot easily calculate the dynamic exponent z with the present approach, because it requires access to the triplet sector, e.g., to extract the spin gap $\Delta \sim L^{-z}$. Our model is explicitly defined only in the singlet sector. While one can extend the VB basis and the projection scheme to triplets,[16,17] the extension of the Q_v and Q_k models to this sector is not unique, and z may depend on how that is accomplished. We could in principle calculate gaps in the singlet sector, but this is much more complicated.

Our main interest in studying the Q_v and Q_k models is in the distribution $P(D_x,D_y)$ of the columnar dimer order parameter. While this is a basis dependent quantity, it still provides direct information on the order parameter symmetry. In a columnar symmetry-broken VBS state, we expect a distribution with a single peak located on the x or y axis, while in a plaquette state the peak should be on one of the 45° rotated axes. In simulations that do not break the symmetry, we expect four-fold symmetric distributions, with peak locations corresponding to the type of VBS as above. In previous studies of VBS states, only ring-shaped distributions were observed,[9–11,14] however, which can be taken as a confirmation of the predicted[7] emergent U(1) symmetry close to a DQCP. One would then expect the fourfold symmetry to appear for large systems, $L \gg \Lambda$, inside the VBS phase, as has been observed explicitly in a classical XY model including dangerously irrelevant Z_q $(q \geq 4)$ perturbations.[15] With the Q_v and Q_k models, we can reach further inside the VBS phases than in the previously studied quantum spin systems, and, as seen in Fig. 4, we can indeed follow the evolution from U(1) to Z_4 symmetric distributions as a function of the coupling constants even for modest system sizes. The peak locations correspond to columnar VBS states for both models, although the shapes of the distributions are qualitative different in other respects. The previously observed ring-shaped distributions[9,14] are more reminiscent of those for the Q_k model.

To study the length scale Λ which governs the $Z_4-U(1)$ crossover (and is related to the scaling dimension of a dangerously irrelevant field[15]) we define an order parameter D_4 which is sensitive to the Z_4 anisotropy,

$$D_4^2 = \int_{-1}^{1} dD_x \int_{-1}^{1} dD_y P(D_x,D_y) r_{xy}^2 \cos(4\theta)$$
$$= \int_0^1 dr \int_0^{2\pi} d\theta r^3 P(r,\theta)\cos(4\theta), \qquad (10)$$

where $r_{xy}=(D_x^2+D_y^2)^{1/2}$. This order parameter should obey the finite-size scaling form;[15,22]

$$D_4^2 = L^{-\sigma_d} F_4(qL^{1/a_4\nu}), \qquad (11)$$

with $a_4>1$. The data can be scaled with $a_4=1.10(4)$, as shown in Fig. 5 (where we use the same Q_v^c, σ_d, and ν as in Figs. 2 and 3). Here, the error bars on the raw data, as seen in the inset, are much larger than for D^2, reflecting that slow

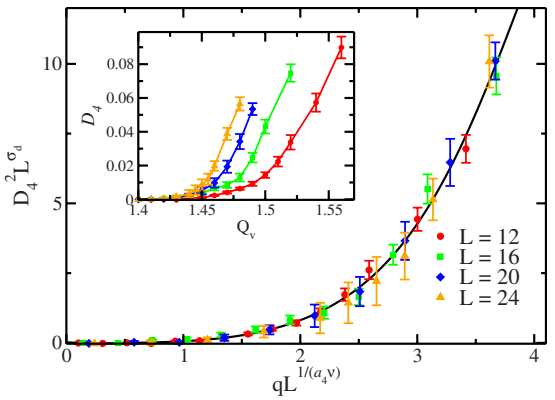

FIG. 5. (Color online) Finite-size scaling of anisotropy order parameter. The inset shows the unscaled data.

angular fluctuations of the VBS order parameter in the simulations (which do not affect the rotationally-invariant D^2). In the classical XY model with Z_4 perturbation[15,23] $a_4 \approx 1.1$, and, thus, the VBS of the Q_v model exhibits similar angular fluctuations. For the Q_k model, the error bars of the D_4 order parameter are much larger and we cannot reliably extract the exponent a_4 in this case.

To summarize, by tuning specific matrix elements in valence-bond QMC simulations, we are able to study a family of SU(2) symmetric states undergoing AF-VBS phase transitions. Unlike previous studies of quantum spin models with VBS states, we are able to observe both the Z_4 symmetry of the order-parameter distribution (which arises from the nature of the VBS on the square lattice) deep inside the VBS phase and the cross-over into an emergent U(1) symmetry upon approaching the transition point. We extracted the length scale Λ, which is found to scale as a power of the correlation length, $\lambda \sim \xi^a$, with $a > 1$, in accord with general expectations for a dangerously irrelevant perturbation (which here is associated with the lattice-imposed fourfold VBS symmetry).[15,22] The critical exponents found here are different from those of the J-Q model,[9,10] which is the best candidate so far for a realization of the DQCP. While our present results are, therefore, most likely not directly related to the particular DQCP theory of Senthil *et al.*,[7] they point to emergent U(1) symmetry as a generic feature of near-critical VBS states.

Signs of Z_4 symmetry in the VBS order parameter were also recently reported for SU(N) symmetric Heisenberg models with large N.[24] The U(1)$-Z_4$ cross-over was not addressed, but could be analyzed with the methods used here. Very recently, the cross-over was observed in generalized J-Q model and the corresponding exponent a_4 was extracted.[25] It is marginally larger (barely outside the error bars) than the value found here.

We would like to thank Naoki Kawashima and Masaki Oshikawa for stimulating discussions. This work was supported by the NSF under Grant No. DMR-0803510.

[1] N. Read and S. Sachdev, Phys. Rev. Lett. **62**, 1694 (1989).
[2] E. Dagotto and A. Moreo, Phys. Rev. Lett. **63**, 2148 (1989); H. J. Schulz, T. Ziman, and D. Poilblanc, J. Phys. I **6**, 675 (1996); L. Capriotti, F. Becca, A. Parola, and S. Sorella, Phys. Rev. Lett. **87**, 097201 (2001).
[3] P. Henelius and A. W. Sandvik, Phys. Rev. B **62**, 1102 (2000).
[4] L. Isaev, G. Ortiz, and J. Dukelsky, Phys. Rev. B **79**, 024409 (2009).
[5] J. Sirker, Z. Weihong, O. P. Sushkov, and J. Oitmaa, Phys. Rev. B **73**, 184420 (2006).
[6] P. W. Anderson, Science **235**, 1196 (1987).
[7] T. Senthil, A. Vishwanath, L. Balents, S. Sachdev, and M. P. A. Fisher, Science **303**, 1490 (2004); M. Levin and T. Senthil, Phys. Rev. B **70**, 220403(R) (2004).
[8] F. S. Nogueira, S. Kragset, and A. Sudbø, Phys. Rev. B **76**, 220403(R) (2007).
[9] A. W. Sandvik, Phys. Rev. Lett. **98**, 227202 (2007).
[10] R. G. Melko and R. K. Kaul, Phys. Rev. Lett. **100**, 017203 (2008); R. K. Kaul and R. G. Melko, Phys. Rev. B **78**, 014417 (2008).
[11] F.-J. Jiang, M. Nyfeler, S. Chandrasekharan, and U.-J. Wiese, J. Stat. Mech. 2008, P02009 (2008).
[12] O. I. Motrunich and A. Vishwanath, arXiv:0805.1494 (unpublished).
[13] A. B. Kuklov, M. Matsumoto, N. V. Prokof'ev, B. V. Svistunov, and M. Troyer, Phys. Rev. Lett. **101**, 050405 (2008).
[14] N. Kawashima and Y. Tanabe, Phys. Rev. Lett. **98**, 057202 (2007).
[15] J. Lou, A. W. Sandvik, and L. Balents, Phys. Rev. Lett. **99**, 207203 (2007).
[16] A. W. Sandvik, Phys. Rev. Lett. **95**, 207203 (2005).
[17] A. W. Sandvik and K. S. D. Beach, in *Computer Simulation Studies in Condensed Matter Physics XX*, edited by D. P. Landau, S. P. Lewis, and H.-B. Schüttler (Springer-Verlag, Berlin, in press); arXiv:0704.1469 (unpublished).
[18] S. Liang, Phys. Rev. B **42**, 6555 (1990).
[19] S. Liang, B. Doucot, and P. W. Anderson, Phys. Rev. Lett. **61**, 365 (1988).
[20] J. Lou and A. W. Sandvik, Phys. Rev. B **76**, 104432 (2007).
[21] S. A. Kivelson, D. S. Rokhsar, and J. P. Sethna, Phys. Rev. B **35**, 8865 (1987); D. S. Rokhsar and S. A. Kivelson, Phys. Rev. Lett. **61**, 2376 (1988).
[22] M. Oshikawa, Phys. Rev. B **61**, 3430 (2000).
[23] J. Manuel Carmona, A. Pelissetto, and E. Vicari, Phys. Rev. B **61**, 15136 (2000).
[24] K. S. D. Beach, F. Alet, M. Mambrini, and S. Capponi, Phys. Rev. B **80**, 184401 (2009).
[25] J. Lou, A. W. Sandvik, and N. Kawashima, Phys. Rev. B **80**, 180414(R) (2009).